Discovery of a new series of jatrophane and lathyrane diterpenes as potent and specific P-glycoprotein modulators†

Elisa Barile,[a] Marianna Borriello,[b] Attilio Di Pietro,[c] Agnès Doreau,[c] Caterina Fattorusso,[b] Ernesto Fattorusso[b] and Virginia Lanzotti*[a]

Received 10th January 2008, Accepted 20th February 2008
First published as an Advance Article on the web 28th March 2008
DOI: 10.1039/b800485d

A new series of diterpenes, the jatrophanes euphoscopin M (**1**), euphoscopin N (**2**) and euphornin L (**3**), and the lathyrane euphohelioscopin C (**7**) were isolated from plants of *Euphorbia helioscopia* L., together with four other known analogues, euphoscopin C (**4**), euphornin (**5**), epieuphoscopin B (**6**) and euphohelioscopin A (**8**). The new compound stereostructures were elucidated by NMR analysis and computational data. The resulting isolated diterpenes were found to be potent inhibitors of P-glycoprotein (ABCB1), while showing an absence of significant activity against BCRP (ABCG2), despite the high substrate overlapping of these transporters, thus including them in the third-generation class of specific multidrug transporter modulators.

Introduction

One of the main reasons for the failure of cancer chemotherapy is the development of multidrug resistance (MDR), whose mechanisms includes the upregulation of membrane-resident transporters effluxing chemotherapeutic drugs out of the tumor cells.[1–3] Several MDR-related drug efflux pumps have been characterized, most of which belong to the superfamily of ATP-binding cassette (ABC) transporters such as P-glycoprotein (Pgp/ABCB1), multidrug resistance-associated protein 1 (MRP1/ABCC1), breast cancer resistance protein (BCRP/ABCG2), and non-ABC transporters such as lung resistance protein (LRP). These proteins may transport either organic anions or neutral organic drugs.[4] As a consequence, Pgp and other MDR proteins have overlapping substrate specificity, *i.e.* drugs can be substrates for several different transporters.[4–6] P-glycoprotein (Pgp) is the best-characterized MDR pump,[7–9] and Pgp-mediated multidrug resistance can be reversed by various inhibitors, including calcium channel blockers, calmodulin antagonists, steroidal agents, immunosuppressive agents, quinolones, indole alkaloids, antibiotics, and detergents.[10] Variability in drug absorption, excessive protein binding, unpredictable plasma levels and unacceptable toxicity have limited their successful development in clinical oncology so far.[11]

First-generation Pgp inhibitors, *e.g.* verapamil, quinidine, and cyclosporine A, lack specificity, require high doses to reverse multidrug resistance, and are associated with unacceptable toxicities.[12–14] Second-generation agents, *e.g.* valspodar, elacridar, biricodar, and dexverapamil, are more potent, specific and less toxic compared to the former inhibitors, but they show interactions with other transporter proteins.[15,16] Third-generation Pgp inhibitors, *e.g.* tariquidar, zosuquidar, laniquidar, and ONT-093, have high potency and specificity for Pgp and in addition have shown no clinically-significant drug interactions with common chemotherapeutic agents.[15,16]

In the search for MDR reversing agents from plants,[17–20] a large number of diterpenes have been isolated from *Euphorbia* spp. that were shown to be potent inhibitors of Pgp, and have constituted an ideal target for SAR studies.

We now report the isolation of four new jatrophane and lathyrane diterpenes, from sun spurge, *Euphorbia helioscopia* L., together with four known analogues.

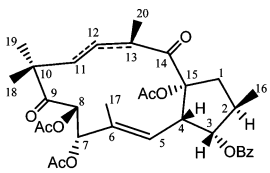

1 $\Delta_{11,12}$
2 $\Delta_{12,13}$

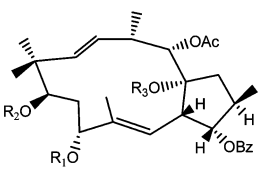

3 $R_1 = H, R_2 = H; R_3 = Ac$
5 $R_1 = Ac, R_2 = Ac; R_3 = H$

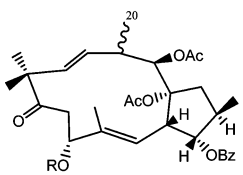

4 R = Bz, 20β
6 R = Ac, 20α

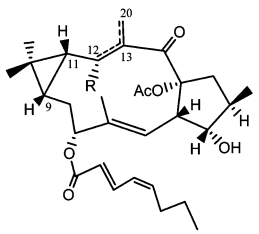

7 R = OH, $\Delta_{13,20}$
8 R = H, $\Delta_{12,13}$

The isolated compounds, individually investigated for their Pgp inhibiting properties, allowed us to get further information on the importance of substitution at positions 7 and 9. The compounds

[a]*DISTAAM, Università degli Studi del Molise, Via F. De Sanctis, I-86100 Campobasso, Italy. E-mail: lanzotti@unimol.it; Fax: +39 874 404652; Tel: +39 874 404649*
[b]*Dipartimento di Chimica delle Sostanze Naturali, Università di Napoli Federico II, Via D. Montesano 49, I-80131 Napoli, Italy*
[c]*Institut de Biologie et Chimie des Proteines, UMR5086 CNRS/ Université Lyon 1 et IFR128 BioSciences Gerland-Lyon Sud, Passage du Vercors 7, 69367 Lyon Cedex 07, France*

† Electronic Supplementary Information (ESI) available: ^{1}H NMR spectra for compounds **1–8**, purity criteria for isolated compounds, and minimum energy conformations obtained for each stereoisomer of **1**. See DOI: 10.1039/b800485d/

are specific inhibitors of Pgp since they show an absence of significant activity against BCRP.

Results and discussion

Chemistry

The EtOAc extract of *E. helioscopia*, collected at the Saepinum ruins (Altilia, Molise, Italy) during April 2004, was filtered through silica gel in order to eliminate gummy compounds. The soluble material was separated using a combination of chromatographic techniques (MPLC and HPLC) eluting with different gradients of EtOAc in hexane to yield compounds **1–8**. Compounds **4–6** and **8** were identified as euphoscopin C (**4**), euphornin (**5**), epieuphoscopin B (**6**) and euphohelioscopin A (**8**), respectively, by comparison of their MS and NMR data with those reported for the original compounds first isolated from samples of *E. helioscopia*,[21] (**4**, **6** and **8**) and *E. maddeni* (**5**).[22] The remaining compounds were new.

The molecular formula of compound **1**, named euphoscopin M, isolated in good yield (32.8 mg), was inferred by HRFABMS as $C_{33}H_{40}O_{10}$. This data, together with its NMR profiles, were indicative of a diterpenoid polyol bearing several ester groups. The nature of the ester groups has been identified by ^{1}H and ^{13}C NMR spectra (Tables 1 and 2) that showed the presence of three acetates and one benzoate. Besides these signals, the ^{1}H and ^{13}C NMR spectra also indicated the presence of five methyls (three singlets and two doublets), two double bonds (one trisubstituted and one *trans*-disubstituted) and four oxygenated sp^3 carbons (three were secondary and one tertiary), all esterified. The remaining oxygenated functions have been ascribed to two ketones by the observation of two characteristic signals at δ_C 205.3 and δ_C 211.2 in the ^{13}C NMR spectrum of **1**.

A 2D HSQC spectrum of **1** allowed the correlation of protons with directly linked carbon atoms. By COSY and HOHAHA techniques the following sequences could be extracted: C-1 to C-5, C-7 and C-8, and C-11 to C-13, including C-20.

Extensive study of the $^{2,3}J_{C-H}$ correlations, obtained from the 2D HMBC spectrum (Fig. 1), allowed the connection of all the above-deduced moieties.

In particular, HMBC correlations of H-4, H-7 and H_3-17 with C-5 connected the first two segments and located the trisubstituted

Table 1 ^{1}H NMR data ($CDCl_3$) of new compounds (**1–3**,**7**) [500 MHz, $CDCl_3$, δ (ppm), mult. and J (Hz)]

H		**1** δ_H (mult., J)	**2** δ_H (mult., J)	**3** δ_H (mult., J)	**7** δ_H (mult., J)
1α		2.58 (dd, 15.0, 8.0)	2.71[a]	1.97[a]	2.53 (dd, 14.0, 9.0)
1β		2.39[a]	2.39[a]	1.80[a]	2.33[a]
2		2.36[a]	2.44[a]	2.18[a]	2.15[a]
3		5.24 (dd, 1.8, 6.2)	5.12 (brs)	5.42 (brs)	3.78 (brs)
4		3.05 (dd, 6.2, 8.0)	3.05 (dd, 7.0, 11.5)	4.96 (dd, 4.5, 10.0)	2.93 (dd, 7.0, 12.0)
5		5.69 (d, 8.0)	5.98 (d, 11.5)	5.71 (d, 10.0)	6.05 (d, 12.0)
7		5.45 (brs)	5.44 (brs)	4.10 (brd)	4.90[a]
8α		5.55 (brs)	5.82 (brs)	2.17[a]	1.73[a]
8β				1.76[a]	2.31[a]
9				4.34 (brd)	0.72 (t, 8.5)
11a		5.43 (d, 16.5)	2.30[a]	5.06 (d, 15.6)	0.88 (t, 8.5)
11b			2.45[a]		
12		5.05 (dd, 9.0, 16.5)	6.45 (brs)	5.63 (dd, 9.6, 15.6)	4.89 (d, 8.0)
13		3.41 (m)		2.61 (brt)	
14				4.94 (bs)	
16		1.24 (d, 6.8)	1.19 (d, 6.8)	0.97 (d, 7.0)	1.13 (d)
17		1.70 (s)	1.65 (s)	1.69 (s)	1.73 (s)
18		1.18 (s)	1.12 (s)	0.95 (s)	1.14 (s)
19		1.33 (s)	1.17 (s)	1.02 (s)	1.13 (s)
20a		1.16 (d, 6.8)	1.77 (s)	0.96 (d, 7.0)	6.39 (s)
20b					5.96 (s)
7-OAc		1.54 (s)	1.59 (s)		
8-OAc		2.10 (s)	2.01 (s)		
14-OAc				2.07 (s)	
15-OAc		2.32 (s)	2.18 (s)	2.22 (s)	2.09 (s)
3-OBz	2,6	8.01 (d, 7.5)	8.06 (d, 7.5)	8.08 (d, 7.5)	
	3,5	7.45 (t)	7.48 (t)	7.44 (t)	
	4	7.58 (t)	7.60 (t)	7.52 (t)	
7-OR	2				5.89 (d, 15.0)
	3				7.61 (dd, 11.9, 15.0)
	4				6.12 (t, 11.9)
	5				5.88[a]
	6a,b				2.29[a]
	7a,b				1.45[a]
	8				0.93 (t, 7.3)

[a] Overlapped by other signals.

Table 2 ^{13}C NMR data ($CDCl_3$) of new compounds (**1–3**,**7**) [125 MHz, $CDCl_3$, δ (ppm) and mult.]

C		**1** δ_C (mult.)	**2** δ_C (mult.)	**3** δ_C (mult.)	**7** δ_C (mult.)
1		42.4 (t)	42.0 (t)	39.7 (t)	41.4 (t)
2		38.9 (d)	38.0 (d)	36.7 (d)	41.1 (d)
3		83.2 (d)	83.3 (d)	81.0 (d)	81.7 (d)
4		50.8 (d)	48.4 (d)	39.6 (d)	50.6 (d)
5		120.5 (d)	122.7 (d)	120.1 (d)	118.8 (d)
6		130.2 (s)	130.2 (s)	130.2 (s)	141.5 (s)
7		73.5 (d)	76.5 (d)	74.6 (d)	76.2 (d)
8		73.5 (d)	73.8 (d)	38.1 (t)	32.1 (t)
9		205.3 (s)	209.1 (d)	78.6 (d)	25.7 (d)
10		49.7 (s)	48.9 (s)	47.9 (s)	41.5 (s)
11		136.3 (d)	39.9 (t)	138.3 (d)	29.0 (d)
12		129.2 (d)	136.4 (d)	128.7 (d)	79.2 (d)
13		45.6 (d)	138.0 (s)	33.8 (d)	148.5 (s)
14		211.2 (s)	197.4 (s)	73.0 (d)	199.5 (s)
15		95.3 (s)	94.3 (s)	94.0 (s)	97.2 (s)
16		18.7 (q)	17.9 (q)	19.7 (q)	18.2 (q)
17		15.8 (q)	16.0 (q)	16.2 (q)	19.0 (q)
18		27.0 (q)	26.4 (q)	22.6 (q)	16.6 (q)
19		22.1 (q)	23.1 (q)	22.7 (q)	18.7 (q)
20		18.4 (q)	12.2 (q)	19.4 (q)	130.2 (t)
7-OAc		20.0 (q)	20.1 (q)		
		168.5 (s)	169.5 (s)		
8-OAc		20.5 (q)	20.5 (q)		
		170.1 (s)	169.5 (s)		
14-OAc				21.0 (q)	
				169.6 (s)	
15-OAc		21.6 (q)	21.6 (q)	21.3 (q)	22.2 (q)
		170.6 (s)	170.1 (s)	171.2 (s)	171.2 (s)
OBz		165.1 (s)	165.4 (s)	165.6 (s)	
	1	130.0 (s)	131.0 (s)	129.9 (s)	
	2,6	129.4 (d)	129.5 (d)	130.0 (d)	
	3,5	128.3 (d)	128.4 (d)	128.6 (d)	
	4	133.0 (d)	133.1 (d)	133.0 (d)	
7-OR	1				166.5 (s)
	2				120.9 (d)
	3				140.1 (d)
	4				126.5 (d)
	5				141.9 (d)
	6a,b				30.2 (t)
	7a,b				22.5 (t)
	8				13.7 (q)

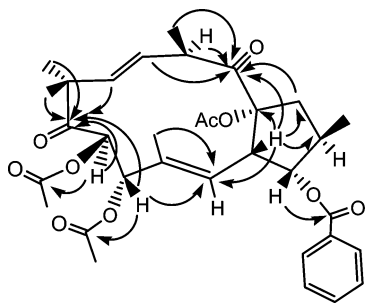

Fig. 1 Selected HMBC correlations exhibited by **1**.

double bond at C-5, while correlations of H-8, H_3-18, H_3-19 and H-11 with C-9 further connected the third spin system to the above-mentioned substructure and placed a ketone at C-9 and the *trans*-disubstituted double bond at C-11. Further correlations of H-12, H-13, H_3-20, H_2-1 and H-4 with C-14, together with a correlation of H-4 with C-15, built the jatrophane skeleton depicted in the formula for **1** and positioned the second keto group at C-14. The correlations of H-3 with the benzoate carbonyl, and of H-7 and H-8 with the acetate carbonyls, ensured the position of the benzoate at C-3 and the acetates at C-7 and C-8, respectively. Consequently, the remaining esterified carbon C-15 must be acetylated, thus fully defining the planar structure of **1**.

The relative stereochemistry of **1** (except C-8 and C-13, see below) was deduced from a series of NOE correlations observed in a ROESY spectrum (Fig. 2).

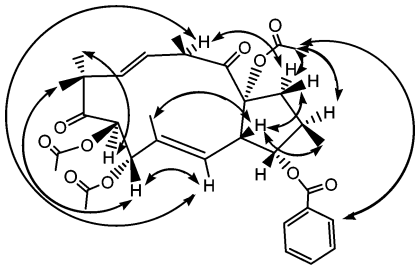

Fig. 2 Selected ROESY correlations exhibited by **1**.

Concerning the stereochemistry of the five-membered ring, NOE effects between H-4–H_3-16 and H-4–H-1β were indicative of their *cis*-relationships, while NOEs between 15-OCH_3–H-1α, 15-OCH_3–H-2 and 15-OCH_3–*ortho*-benzoyl protons determined their *cis*-orientations. These data secured the relative configuration of the five-membered ring. Concerning the stereochemistry of the medium sized ring, in the ^1H NMR spectrum we observed that the protons of the acetyl group at C-7 are strongly shifted upfield (δ_H 1.54). This feature was already found in other jatrophane analogues,[23,24] and was explained as due to the anisotropic effect of the *cis*-located benzoate ester group at C-3. Therefore, we could also confidently assume a *cis*-relationship of the substituents at C-3 and C-7 in compound **1**. The *E* stereochemistry of the C-11–C-12 double bond has been defined on the basis of the coupling constant between H-11 and H-12 ($J = 16.5$ Hz).

Concerning the geometry of the C-5–C-6 double bond, NOEs between H-5–H-7 and H_3-17–H-4 defined its *E* configuration.

In order to assign the absolute configuration at the C-8 and C-13 atoms, we integrated the NMR data with a thorough computational analysis performed on the four possible stereoisomers of **1** (8*R*,13*R*; 8*S*,13*R*; 8*R*,13*S*; 8*S*,13*S*). In particular, each stereoisomer was subjected to a molecular dynamic (annealing) simulation in order to properly sample its conformational space (Discover 3 module, Insight 2005). The resulting conformations were energy minimized and structurally optimized by means of molecular mechanics and AM1 semiempirical calculations (MOPAC module of Insight 2001, see Experimental). The obtained conformers were grouped into structurally related families and filtered on the basis of the NMR data (Fig. S1, ESI†).

Firstly, our results indicated that the intense dipolar coupling between H-5 and H-13 observed by ROESY NMR, is possible only when the configuration at C-13 is *R*, consequently restricting our research to the two remaining stereoisomers (i.e. 8*R*,13*R* and 8*S*,13*R*). Subsequently, our analysis highlighted that only the 8*S*,13*R* stereoisomer could fit all the experimental NMR data obtained (Fig. 3 and S1), such as i) the very low value of $J_{H\text{-}7\text{–}H\text{-}8}$ (<1.5 Hz), indicating a dihedral angle close to 90°, in the range 70–110°; ii) the remarkable NOE correlation between: H-5 and H-13; H-5 and the hydrogen atoms in the *ortho* position of the

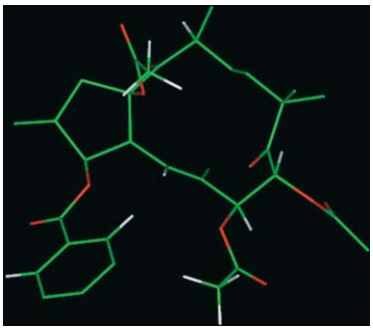

Fig. 3 Fully optimized AM1 conformer of the 8*S*,13*R* stereoisomer of euphoscopin M (**1**). Atoms are colored by atom type: carbon = green; oxygen = red; hydrogen = white. Hydrogen atoms, with the exceptions of those useful for the NMR discussion, are omitted for clarity of presentation.

benzene ring; H-5 and the hydrogens of the acetylic group at C-15; iii) the above mentioned *cis* relationships between C-3 and C-7 substituents.

Interestingly, our computational results evidenced that the experimentally observed interaction between the hydrogens of the acetyl group at C-7 and the electron rich benzene ring at C-3, resulting in the remarkable upfield shift of the acetoxy methyl protons, is related to the H-7–H-8 dihedral angle value. In fact, two low energy conformers of the 8*S*,13*R* stereoisomer of **1** were selected (Fig. S2) both with H-7–H-8 dihedral angle values in the range 70–110°, but only the green conformer (Fig. 3 and S2), with a dihedral angle of 70°, also showed an optimized interaction between the protons of the acetyl group at C-7 and the aromatic ring at C-3. Weak NOE correlations between H-1α–H-13, H_3-18–H-7 and H_3-19–H-8 (Fig. 2) further supported the resulting stereochemical assignment. It has to be noted that our data allowed us to assign the relative configuration of compound **1**. However, we can assume its absolute configuration to be as depicted in the formula considering that all the jatrophanes so far isolated from *Euphorbia* species invariably have the *S* configuration at C-4.[23,24]

Compounds **2**, **3** and **7** are closely related to **1** and to the other known isolated compounds (**4–6**, and **8**). Consequently, the stereostructure elucidation of these molecules was greatly aided by the comparison of their spectroscopic data with those obtained for **1** and for the other known isolated compounds (**4–6**, and **8**). Even so, it should be noted that a complete set of 2D NMR spectra (COSY, HSQC, HMBC) was acquired for each metabolite in order to gain the complete and unambiguous assignment of the ^{1}H and ^{13}C NMR resonances as listed in Tables 1 and 2, respectively. The same relative stereochemistry previously assigned to **1** was also confirmed for **2** and **3** by 2D NMR ROESY spectroscopy.

Compound **2**, named euphoscopin N, was isolated in good yield (16.4 mg), and by HRFABMS spectrum showed the same molecular formula as **1**. The NMR spectra of **2** (Tables 1 and 2) revealed close similarities with those of **1** and showed the missing of signals to be due to the *trans*-disubstituted double bond at C-11. This, together with the downfield shift of H_3-20 (singlet at δ_H 1.77 in **2** *vs.* doublet at δ_H 1.16 in **1**) suggested an isomerization of the double bond at C-12 that has been confirmed by the ^{1}H and ^{13}C NMR resonances of the relative protons and carbons [^{1}H: δ_H 2.30 and δ_H 2.45 (H_2-11), δ_H 6.45 (H-12); ^{13}C: δ_C 39.9 (C-11), δ_C 136.4 (C-12), δ_C 138.0 (C-13)].

Compound **3**, named euphornin L, $C_{31}H_{42}O_8$ by HRFABMS, was isolated in low amounts as a colorless amorphous solid. Analysis of its ^{1}H and ^{13}C NMR spectra (Tables 1 and 2) indicated the same core structure as **5**, and revealed the presence of two acetyls and a benzoyl group. HMBC cross peaks of H-3 (δ_H 5.42 brs) with the carbonyl of the benzoate (δ_C 165.6) and of H-14 with the carbonyl of an acetate (δ_C 169.6), indicated the linkage of the benzoyl and an acetyl at C-3 and C-14, respectively. The second acetyl group has been located at C-15 because of its characteristic deshielded chemical shift value (3H, s, δ_H 2.22) in the ^{1}H NMR spectrum. As a consequence, the other oxygenated functionalities required by the molecular formula have been ascribed to two hydroxyl groups, located on the remaining oxygenated carbons C-7 and C-9 [upfield shifted protons at δ_H 4.10 (H-7) and δ_H 4.34 (H-9)].

Compound **7**, named euphohelioscopin C, isolated in low amounts (1.1 mg), had the formula $C_{30}H_{42}O_7$ determined by HRFABMS, differing from that of **8** by the presence of one additional oxygen atom. Its NMR spectrum showed the following remarkable differences when compared to that of compound **8**: i) the absence of the characteristic H_3-20 resonance (δ_H 1.84 in **8**) and the presence of an exomethylene (δ_H 5.96 and δ_H 6.39 in **7**); ii) an upfield shift of H-12 (δ_H 4.89 in **7** *vs.* δ_H 6.60 in **8**). A combined analysis of the 2D COSY, HSQC and HMBC spectra allowed us to define the core structure of compound **7**, with the only changes being confined to the presence of one additional hydroxyl group at C-12 and the shift of the double bond to C-13–C-20. As a consequence, in the ^{13}C NMR spectra of **7** signal C-12 resonated in the region of oxygen-bearing carbons (doublet at δ_C 79.2). In addition, the vicinal coupling constant (J = 8.5 Hz) between the protons H-9 and H-11 of the cyclopropane ring suggested that they are *cis*-oriented. NOE correlations of H-12 with H_3-17, H-9 and H-11 confirmed this structural feature and also indicated an α-orientation of the hydroxyl group at C-12 respectively. The ^{1}H and ^{13}C NMR assignments of **7** are reported in Tables 1 and 2.

Only four of the previously described jatrophane and lathyrane diterpenes, compounds **4–6** and **8**, were isolated in the plant material analyzed. The differences observed, between this and previous work,[21,23–25] in the composition of the diterpene mixture obtained from the same plant species, are likely to be related to the different geographical origins and environmental conditions of the samples (Central Italy and Japan, respectively).

Biological evaluation

The biological activity of the isolated jatrophane (**1**, **2**, **4**, **5** and **6**) and lathyrane (**8**) diterpenes was monitored through their ability to inhibit P-glycoprotein-mediated mitoxantrone efflux leading to drug accumulation, as measured by flow cytometry.

Fig. 4 shows that all the compounds exhibited a concentration-dependent inhibition of mitoxantrone efflux, finally reaching a maximal effect. The concentration dependence analysis indicated that compound **6** (the jatrophane epieuphoscopin B) was twice as potent as the reference inhibitor cyclosporin A, with an IC_{50} of 1.71 ± 0.83 μM (as illustrated in Fig. 5) in comparison with 3.37 ± 1.39 μM.

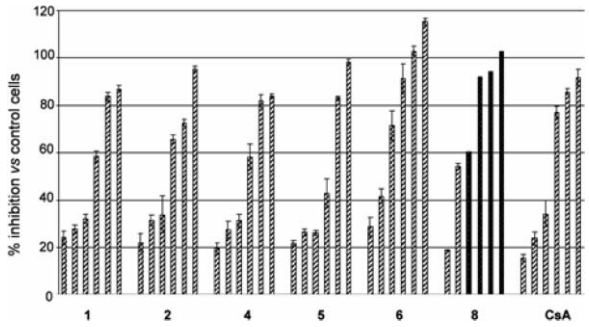

Fig. 4 Concentration-dependent inhibition of Pgp-mediated mitoxantrone efflux by the purified compounds. MDR1-transfected cells and parental ones were first incubated with mitoxantrone and then with each purified inhibitor. Compounds were tested at concentrations of 0, 0.5, 2.0, 2.5, 10, 20 μM, except compound **8**, which was tested at 0, 20, 40, 60, 80, 100 μM (results obtained at the last four concentrations are shown in bold because these concentrations were different from those used in the other experiments). Mitoxantrone accumulation was assayed by flow cytometry, and the inhibition efficiency was determined as reported in the experimental section. Cyclosporin A (CsA) was used as a reference inhibitor.

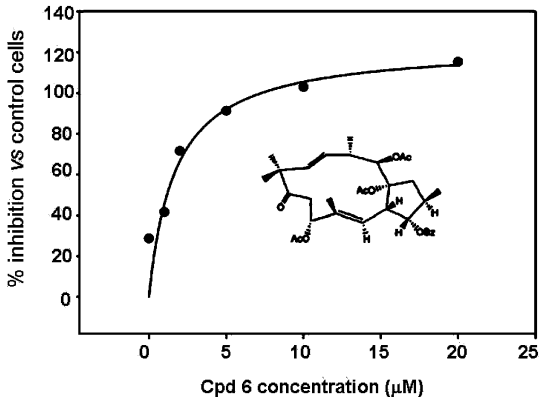

Fig. 5 Determination of the IC_{50} value for the best inhibitor. The inhibition data were obtained as in Fig. 4 for epieuphoscopin B (**6**), whose chemical structure is shown, and analyzed with the Sigma Plot 8.0 software.

In contrast, compounds **5** and **8** were much less efficient, with IC_{50} values of 8.46 ± 3.51 μM and 14.0 ± 2.4 μM respectively. In the latter case, concerning the lathyrane euphohelioscopin A, a very high concentration of 100 μM was required to get maximal inhibition. Finally, the remaining compounds **1**, **2** and **4** appeared similar in activity to cyclosporin A, with IC_{50} values of 3.78 ± 2.18 μM, 3.47 ± 1.88 μM and 3.58 ± 1.78 μM respectively.

Three main structure–activity relationships for P-glycoprotein inhibition could be drawn for the substituents from the differential inhibitory effects observed: i) a marked, 5-fold, positive effect played by a carbonyl *versus* an OAc group at position 9 when comparing compounds **6** and **5**, ii) a 2-fold positive effect of an OAc *versus* an OBz substituent at position 7 when comparing compounds **6** and **4**, and iii) a neutral effect of having the double bond at either 11–12 or 12–13 positions in compounds **2** and **1**. This new important information resulting from the comparison of jatrophanes isolated from *E. helioscopia* is complementary to that previously drawn from jatrophanes isolated from other *Euphorbiae* species.[17–20]

Interestingly, the same compounds were not able to alter the mitoxantrone efflux mediated, under similar conditions, by the other multidrug transporter ABCG2 (Fig. 6). Indeed, no significant inhibition was observed for any compound up to a 20 μM concentration, whereas the control inhibitor GF120918 gave a submicromolar IC_{50} value, in agreement with previous observations.[26,27]

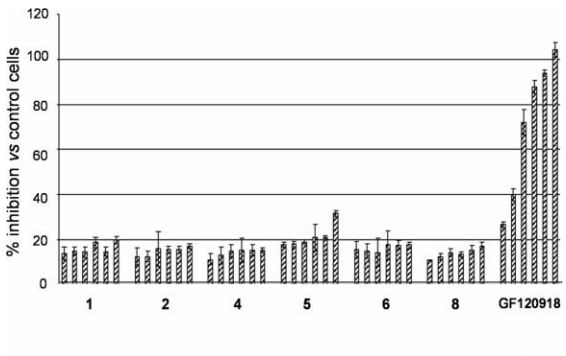

Fig. 6 Concentration-dependent inhibition of ABCG2-mediated mitoxantrone efflux by the purified compounds. ABCG2-transfected cells and parental ones were incubated with mitoxantrone and then with each purified inhibitor at increasing concentrations of 0.1, 0.5, 2. 5, 10 and 20 μM. Mitoxantrone accumulation was assayed and the inhibition efficiency determined as in Fig. 4. GF120918 was used as a reference inhibitor.

Such a specificity towards P-glycoprotein was observed with other types of inhibitors, such as amiodarone, nifedipine, dexniguldipine, LY335979 (Zosuquidar) and R101933 (Laniquidar) as reviewed.[28] Conversely, other types of inhibitors, such as fumitremorgin C, Ko143, tectochrysin and 6-prenylchrysin, were found to selectively inhibit ABCG2 and not P-glycoprotein.[26,27]

All these compounds, belonging to the third-generation class of specific multidrug transporter inhibitors, constitute convenient and efficient tools for evaluating the contribution of each transporter to cell drug efflux and related multidrug resistance phenotypes, in various cell lines or tissues under either normal or pathological conditions. Future clinical trials will evaluate the clinical benefit of these recently-discovered compounds.

Experimental

General experimental procedures

Optical rotations were determined on a Perkin Elmer 192 polarimeter equipped with a sodium lamp (589 nm) and 10 cm microcell. ^1H (500 MHz) and ^{13}C (125 MHz) NMR spectra were recorded on a Varian Unity INOVA spectrometer; chemical shifts were referred to the residual solvent signal ($CDCl_3$: δ_H 7.26, δ_C 77.0). The multiplicities of ^{13}C NMR resonances were determined by DEPT experiments. ^1H connectivities were determined by using COSY experiments; one-bond heteronuclear ^1H–^{13}C connectivities were determined with a 2D HSQC pulse sequence with an interpulse delay set for $^1J_{C\text{–}H}$ of 130 Hz. Two and three bond heteronuclear ^1H–^{13}C connectivities were determined with 2D NMR HMBC experiments, optimized for a $^{2,3}J_{C\text{–}H}$ of 8 Hz. The measurement of spatial coupling was obtained through 2D ROESY experiments. Low-resolution electrospray

(positive ion) mass spectra were performed employing an API 2000 spectrometer; high-resolution FAB mass spectra (glycerol matrix) were measured on a VG ProSpec (FISONS) mass spectrometer. Medium pressure liquid chromatography (MPLC) was performed on a Büchi 861 apparatus using silica gel (230–400 mesh) as the stationary phase. HPLC in isocratic mode was performed on a Varian apparatus equipped with an RI-3 refractive index detector using Merck columns [semipreparative LiChrocart Si60 column (10 μ) with a flow rate of 2.5 mL min^{-1} and analytical LiChrospher Si60 (5 μ) with a flow rate of 1 mL min^{-1}].

Plant material, extraction and isolation

Samples of *Euphorbia helioscopia* L. were collected at the Saepinum ruins, Altilia (CB) during April 2004. A voucher specimen is kept at the Department of STAAM, Campobasso. Fresh whole plants (3.5 kg, fresh plant), including latex and roots, were extracted seven times with 3.5 L of EtOAc at room temperature. This extract (44.3 g) was partitioned between H_2O and EtOAc, in order to remove hydrophilic and gummy compounds, and then the sole apolar fraction (24.9 g) was chromatographed by MPLC on silica gel column (230–400 mesh) using a gradient solvent system from hexane 100% to EtOAc 100%. Preliminary NMR studies revealed that three fractions, eluted in hexane–EtOAc (7 : 3), hexane–EtOAc (6 : 4) and hexane–EtOAc (55 : 45), contained diterpenoids of the jatrophane and lathyrane family and were further investigated. The first fraction, hexane–EtOAc (7 : 3), was first purified by a semipreparative HPLC direct phase column, using hexane–EtOAc (85 : 15) as the mobile phase, affording the known compound **4** (17.3 mg). The second fraction, hexane–EtOAc (6 : 4), after purification on a semipreparative HPLC direct phase column with hexane–EtOAc (75 : 25) as the eluent, afforded compounds **1** (32.8 mg), **5** (31.5 mg), and **8** (36.5 mg) in a pure form together with a fraction that was further separated on an analytical column, with a mobile phase of hexane–EtOAc (8 : 2), giving the known compound **6** (17.3 mg). The last fraction, hexane–EtOAc (55 : 45) was chromatographed on a semipreparative HPLC direct phase column, using hexane–EtOAc (7 : 3) as the system solvent, affording three fractions which needed to be further purified. Therefore they were purified separately on an analytical column eluting with hexane–EtOAc (7 : 3) for the first fraction and eluting with hexane–EtOAc (75 : 25) for both the remaining ones: compounds **3** (0.6 mg), **2** (16.4 mg), and **7** (1.1 mg) respectively were obtained.

Euphoscopin M (1). Colorless amorphous solid; $[\alpha]_D^{25}$ +11.4 (*c* 0.01 in $CHCl_3$); ν_{max} (KBr)/cm^{-1} 3448, 1750, and 1480; ESIMS (positive ion) *m/z* 619 $[M + Na]^+$; HRFABMS (positive ion): found *m/z* 597.6730 (calcd for $C_{33}H_{41}O_{10}$, *m/z* 597.6725); ^1H NMR (500 MHz, $CDCl_3$): see Table 1; ^{13}C NMR (500 MHz, $CDCl_3$): see Table 2.

Euphoscopin N (2). Colorless amorphous solid; $[\alpha]_D^{25}$ +31.4 (*c* 0.01 in $CHCl_3$); ν_{max} (KBr)/cm^{-1} 3450, 1748, and 1480; ESIMS (positive ion) *m/z* 619 $[M + Na]^+$; HRFABMS (positive ion): found *m/z* 596.6729 (calcd for $C_{33}H_{41}O_{10}$, *m/z* 597.6725); ^1H NMR (500 MHz, $CDCl_3$): see Table 1; ^{13}C NMR (500 MHz, $CDCl_3$): see Table 2.

Euphornin L (3). Colorless amorphous solid; $[\alpha]_D^{25}$ +27.4 (*c* 0.01 in $CHCl_3$); ν_{max} (KBr)/cm^{-1} 3450, 1749, and 1479; ESIMS (positive ion) *m/z* 565 $[M + Na]^+$; HRFABMS (positive ion): found *m/z* 543.6686 (calcd for $C_{31}H_{43}O_8$, *m/z* 543.6682); ^1H NMR (500 MHz, $CDCl_3$): see Table 1; ^{13}C NMR (500 MHz, $CDCl_3$): see Table 2.

Euphohelioscopin C (7). Colorless amorphous solid; $[\alpha]_D^{25}$ +32.4 (*c* 0.01 in $CHCl_3$); ν_{max} (KBr)/cm^{-1} 3449, 1750, and 1480; ESIMS (positive ion) *m/z* 537 $[M + Na]^+$; HRFABMS (positive ion): found *m/z* 515.6586 (calcd for $C_{30}H_{43}O_7$, *m/z* 515.6581); ^1H NMR (500 MHz, $CDCl_3$): see Table 1; ^{13}C NMR (500 MHz, $CDCl_3$): see Table 2.

Molecular modeling calculations

Molecular modeling calculations were performed on an SGI Origin 200 8XR12000, while the molecular modeling of graphics was carried out on SGI Octane 2 and Octane workstations. Compound **1** was built using the Insight 2005 Builder module (Accelrys, San Diego). Molecular mechanics (MM) and dynamics (MD) calculations were performed using the atomic potentials and charges assigned by the cff91 force field,[29] while semi-empirical calculations were performed using the Mopac 6.0 package.[30] The conformational space of the compounds was sampled through 200 cycles of simulated annealing (Discover 3 module of Insight 2005). An initial temperature of 1000 K was applied to the system for 1000 fs with the aim of surmounting torsional barriers; the temperature was then linearly reduced to 200 K with a decrement of 0.5 K fs^{-1} (time step = 1.0 fs). The resulting structures were subjected to energy minimization within the Insight 2005 Discover 3 module (cff91 force field, conjugate gradient algorithm[31]) until the maximum RMS derivative was less than 0.001 kcal $Å^{-1}$. All calculations were performed using a $CHCl_3$ dielectric constant of 4.806. Successively, the MD–MM conformers were subjected to a full geometry optimization by semiempirical calculations, using the quantum mechanical method AM1 in the Mopac 6.0 package in the Ampac/Mopac module of Insight 2000.1. The GNORM value was set to 0.5. To reach a full geometry optimization the criteria for terminating all optimizations was increased by a factor of 100, using the keyword PRECISE. The resulting structures were ranked by their conformational energy values and grouped into families according to their dihedral angle values. Using the NMR data, distances between the coupled hydrogens as well as spatial relationships evidenced by NOE effects were calculated and tabulated for the subsequent analysis.

Biological assays

In the case of P-glycoprotein, cell lines were commercially obtained from ATCC: NIH3T3 (SD no. 1825), the drug-sensitive parental cell line, is a continuous line of contact-inhibited cells derived from NIH Swiss mouse embryo cultures, whereas the multidrug-resistant cell line NIH-MDR-G185 (SD no. 1823) is a clone of NIH3T3 cells transfected with the wild-type pHaMDR1/A (G185) retroviral vector by the calcium phosphate co-precipitation method, and maintained in the presence of 60 ng ml^{-1} colchicine, as described.[32] The parental and transfected cells were grown in monolayer at 37 °C in 5% CO_2 using DMEM (Whittaker BioProducts) supplemented with 10% fetal bovine serum, 5 μM glutamine, 580 units ml^{-1} penicillin and 50 μg ml^{-1} streptomycin (GIBCO). For the flow cytometry assays of mitoxantrone efflux, 1×10^5 cells were incubated with 5 μM mitoxantrone for 60 min

at 37 °C, with or without inhibitors, and washed twice in ice-cold saline buffer. Mitoxantrone-derived fluorescence of 10,000 events was measured through a 488 nm bandpass filter at an excitation wavelength of 650 nm, using a FACscan flow cytometer (Becton Dickinson). The mitoxantrone accumulation after incubation for 30 min was expressed in fluorescence units (FU). Parallel experiments were performed at each inhibitor concentration with both cell lines, and in the absence of mitoxantrone to determine autofluorescence. The P-glycoprotein-mediated efflux activity was measured as the difference between the residual mitoxantrone accumulation in the transfected cells relative to the maximal value observed in the parental cells. The efflux inhibition by cyclosporin A and the purified compounds increased the residual accumulation up to the level of the parental cells. Data are the mean of two independent experiments.

Concerning ABCG2, HEK293 cells were maintained at 37 °C, with 5% CO_2 in Dulbecco's modified Eagle's medium (DMEM) supplemented with 10% fetal bovine serum, 5 μM glutamine, 580 units ml^{-1} penicillin, and 50 μg ml^{-1} streptomycin. For stable transfection, the HEK293 cells were seeded in a 10 μg ml^{-1} poly-D-lysine coated 60 mm^2 petri dish one day before, and 8 μg pcDNA3.1-ABCG2 was added using the Fecturin™/Polyplus transfection system (Ozyme). A stably-transfected pool clone was selected using Geneticin (G418) at 0.8 mg ml^{-1}. For inhibition of ABCG2-mediated mitoxantrone efflux, 1×10^5 cells were incubated for 1 h at 37 °C in 200 μL of DMEM medium and assayed by flow cytometry under similar conditions as described for P-glycoprotein-transfected cells, except that GF120918 was used as the reference inhibitor.

Conclusion

A new series of diterpenes based on jatrophane (**1–3**) and lathyrane (**7**) skeletons was isolated, together with four other known analogues, euphoscopin C (**4**), euphornin (**5**), epieuphoscopin B (**6**) and euphohelioscopin A (**8**) from whole plants of *Euphorbia helioscopia* L. Their stereostructures were elucidated with the aid of extensive NMR analysis supported by a thorough molecular investigation based on molecular dynamics, mechanics, and semiempirical calculations. The isolated compounds exhibited *in vitro* activity as inhibitors of P-glycoprotein (ABCB1). Among them, epieuphoscopin B (**6**) behaved as the most potent inhibitor of mitoxantrone efflux activity, being twice as efficient as the reference inhibitor cyclosporin A. Structure–activity relationships among jatrophanes showed the importance of substitution at positions 7 and 9. Interestingly, these compounds appear to be specific P-glycoprotein inhibitors since they show an absence of significant activity against BCRP (ABCG2), despite the high substrate overlapping of these transporters, thus including them in the third-generation class of specific multidrug transporter modulators. Future clinical trials will evaluate the clinical benefits of these recently discovered compounds.

Acknowledgements

This work was supported by Italian FIRB 2003-RBNE03B8K and French ARC 3942 and ANR-06-BLAN-0420. We thank Mr. R. Troiano and Dr B. Zolfaghari for collecting and identifying the plant material. Mass and NMR spectra were recorded at CSIAS, University of Naples Federico II. Flow cytometry experiments were performed at IFR128, Gerland-Lyon Sud.

References

1 M. I. Borges-Walmsley, K. S. McKeegan and A. R. Walmsley, *Biochem. J.*, 2003, **376**, 313338.
2 S. M. Sisodiya, *Curr. Opin. Neurol.*, 2003, **16**, 197–201.
3 G. Jansen, R. J. Scheper and B. A. Dijkmans, *Scand. J. Rheumatol.*, 2003, **32**, 325–336.
4 P. Borst, R. Evers, M. Kool and J. Wijnholds, *J. Natl. Cancer Inst.*, 2000, **92**, 1295–1302.
5 A. Seelig, X. L. Blatter and F. Wohnsland, *Int. J. Clin. Pharmacol. Ther.*, 2000, **38**, 111–121.
6 H. Schinkel and J. W. Jonker, *Adv. Drug Delivery Rev.*, 2003, **55**, 3–29.
7 R. L. Juliano and V. Ling, *Biochim. Biophys. Acta*, 1976, **455**, 152–162.
8 J. H. Gerlach, J. A. Endicott, P. F. Juranka, G. Henderson, F. Sarangi, K. L. Deuchars and V. Ling, *Nature*, 1986, **324**, 485–489.
9 P. Gros, J. Croop and D. Housman, *Cell*, 1986, **47**, 371–380.
10 D. R. Ferry, H. Traunecker and D. J. Kerr, *Eur. J. Cancer*, 1996, **32A**, 1070–1081.
11 P. Sonneveld and A. F. List, *Best Pract. Res. Clin. Haematol.*, 2001, **14**, 211–233.
12 P. Marie, J. N. Bastie, F. Coloma, A. M. F. Suberville, A. Delmer, B. Rio, B. Delmas-Marsalet, G. Leroux, P. Casassus, E. Baumelou, J. Catalin and R. Zittoun, *Leukemia*, 1993, **7**, 821–824.
13 E. Solary, D. Caillot, B. Chauffert, R. O. Casasnovas, M. Dumas, M. Maynadie and H. Guy, *J. Clin. Oncol.*, 1992, **10**, 1730–1736.
14 A. Doyle and D. D. Ross, *Oncogene*, 2003, **22**, 7340–7358.
15 S. F. Bates, C. Chen, R. Robey, M. Kang, W. D. Figg and T. Fojo, *Novartis Found Symp.*, 2002, **243**, 83–96.
16 H. Thomas and H. M. Coley, *Cancer Control*, 2003, **10**, 159–165.
17 G. Corea, E. Fattorusso, V. Lanzotti, O. Taglialatela-Scafati, G. Appendino, M. Ballero, P. N. Simon, C. Dumontet and A. Di Pietro, *J. Med. Chem.*, 2003, **46**, 3395–3402.
18 G. Corea, E. Fattorusso, V. Lanzotti, O. Taglialatela-Scafati, G. Appendino, M. Ballero, P. N. Simon, C. Dumontet and A. Di Pietro, *Bioorg. Med. Chem.*, 2003, **11**, 5221–5227.
19 G. Corea, E. Fattorusso, V. Lanzotti, R. Motti, P. N. Simon, C. Dumontet and A. Di Pietro, *J. Med. Chem.*, 2004, **47**, 988–992.
20 G. Corea, E. Fattorusso, V. Lanzotti, R. Motti, P. N. Simon, C. Dumontet and A. Di Pietro, *Planta Med.*, 2004, **70**, 657–665.
21 Yamamura, Y. Shizuri, S. Kosemura, J. Ohtsuka, T. Tayama, S. Ohiba, M. Ito, Y. Saito and Y. Terada, *Phytochemistry*, 1989, **28**, 3421–3436.
22 R. Sahai, R. P. Rastogi, J. Jakupovic and F. Bohlmann, *Phytochemistry*, 1981, **20**, 1665–1667.
23 S. Yamamura, S. Kosemura, S. Ohba, M. Ito and Y. Saito, *Tetrahedron Lett.*, 1981, **22**, 5315–5318.
24 Y. Shizuri, S. Kosemura, J. Ohtsuka, Y. Terada and S. Yamamura, *Tetrahedron Lett.*, 1983, **24**, 2577–2580.
25 Y. Shizuri, S. Kosemura, J. Ohtsuka, Y. Terada, S. Yamamura, S. Ohba, M. Ito and Y. Saito, *Tetrahedron Lett.*, 1984, **25**, 1155–1158.
26 A. Ahmed-Belkacem, A. Pozza, F. Munoz-Martinez, S. E. Bates, S. Castanys, F. Gamarro, A. Di Pietro and J. M. Perez-Victoria, *Cancer Res.*, 2005, **65**, 4852–4860.
27 A. Ahmed-Belkacem, A. Pozza, S. Macalou, J. M. Perez-Victoria, A. Boumendjel and A. Di Pietro, *Anti-Cancer Drugs*, 2006, **17**, 239–243.
28 G. Szakacs, J. K. Paterson, J. A. Ludwig, C. Booth-Genthe and M. M. Gottesman, *Nat. Rev. Drug Discovery*, 2006, **5**, 219–234.
29 J. R. Maple, U. Diniur and A. T. Hagler, *Proc. Natl. Acad. Sci. U. S. A.*, 1988, **85**, 5350–5354.
30 J. J. P. Stewart, *J. Comput. Aided Mol. Des.*, 1990, **4**, 1–105.
31 R. Fletcher, *Practical Methods of Optimization*, J. Wiley & Sons, New York, 1980, vol.1.
32 O. Cardarelli, I. Aksentijevich, I. Pastan and M. Gottesman, *Cancer Res.*, 1995, **55**, 1086–1091.

